SAND--91-0039C

DE91 014105

# SHOCK-WAVE PROPERTIES OF HIGH-STRENGTH CERAMICS

Dennis GRADY

Sandia National Laboratories, Impact Physics Division 1543, P. O. Box 5800, Albuquerque, New Mexico, 87185-5800

The shock and release response of a suite of high-strength ceramics has been investigated with controlled planar impact methods and velocity interferometry diagnostics. The study provides Hugoniot, yield and post-yield compressive strength, phase transformation and tensile spall material properties data for these ceramics.

## 1. INTRODUCTION

Certain of the intermetallic light weight compounds in polycrystalline ceramic form exhibit some of the highest strength properties measured on engineering materials. Limited plastic slip systems in these materials preclude lower stress plastic flow and dynamic strengths approach an appreciable fraction of their theoretical strengths[1].

Post-yield dynamic deformation of these ceramics is not understood. Although pervasive fine scale cataclastic fracture has generally been favored in material modelling[2], plastic flow through dislocation slip under the large confining pressures experienced in shock compression, either homogeneous or heterogeneous, cannot be ruled out.

Further, response to transient loads in these materials can be complicated by pressure induced phase transformation. Because of the high dynamic yield strengths, phase transformation and yield can intermix, placing more stringent requirements on material response models.

In the present investigation, dynamic material properties of high-strength ceramics have been studied using controlled impact methods. In the work reported, planar impact experiments, using high-resolution velocity interferometry diagnostics, have been performed on six ceramics. The materials investigated are aluminum nitride, aluminum oxide, boron carbide, silicon carbide, titanium diboride and zirconium dioxide. Planar shock and release experiments have been performed to investigate Hugoniot properties, dynamic yield and post yield behavior, phase transformation, release equation of state and tensile spall characteristics. Peak impact stresses range from below the Hugoniot elastic limit to approximately 60 GPa. Material property results are extracted from measured wave profile data through analytic and computational methods.

## 2. EXPERIMENTAL STUDIES

High-strength ceramics tested in the present program have been acquired from a number of sources. In several cases the same ceramic from several suppliers has been investigated allowing insightful comparisons of material properties variations due to differences in impurity content, microstructure and ceramic preparation.

In the present experimental study, gun impact methods and velocity interferometry (VISAR) diagnostics[3] are used to measure compression and release velocity profiles at an interface between the ceramic and a lithium fluoride window. The primary experimental results are the time-resolved interface velocity profiles. These profiles are used individually and collectively through both computational and analytic methods to extract desired dynamic critical material property data.

## 3. DYNAMIC MATERIAL PROPERTIES

Measured visar wave profiles are used to determine material property data for ceramics under the high confining pressures and deformation strain rates experienced during uniaxial strain impact loading. This study

*This work performed at Sandia National Laboratories supported by the U.S. DOE under contract #DE-AC04-76DP00789.

---

has provided material property data on ceramics for the Hugoniot response, Hugoniot elastic limit, post-yield strength, shock release and tensile spall. Results of this study are summarized below.

3.1 Hugoniot Response

Principal Hugoniot data for the six high strength ceramics determined from the primary data are shown in Figure 1. Small differences in Hugoniot behavior for the same ceramic from different suppliers are not indicated here. Steeper behavior of titanium diboride and zirconium dioxide reflect the higher density of these ceramics; approximately 4500 kg/m$^3$ for titanium diboride and 6000 kg/m$^3$ for zirconium dioxide. The shallow trend of the aluminum oxide corresponds to the large porosity of the particular material investigated in this study. Softening of the Hugoniots for aluminum nitride and boron carbide above about 15 to 20 GPa is related to phase transformation in the former and catastrophic loss of strength in the latter.

3.2 Hugoniot Elastic Limit

The Hugoniot elastic limit (HEL) identifies the axial stress at which a solid, loaded in compression under constraint of uniaxial strain, can no longer support elastic distortion and begins to flow through plastic or cataclastic fracture processes. HEL data determined from the present wave profile experiments are summarized in Figure 2. For each material the reported HEL is

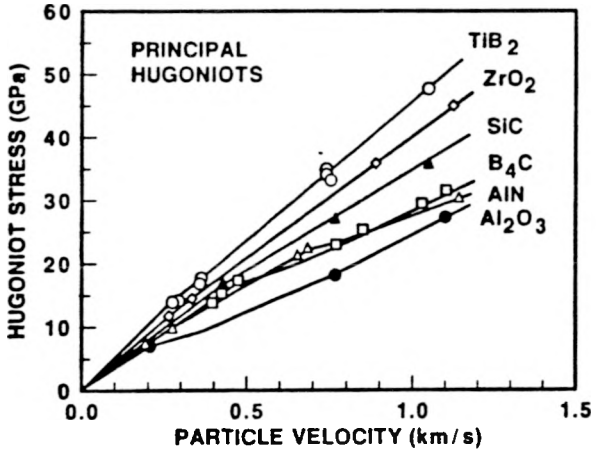


FIGURE 1

Hugoniot properties.

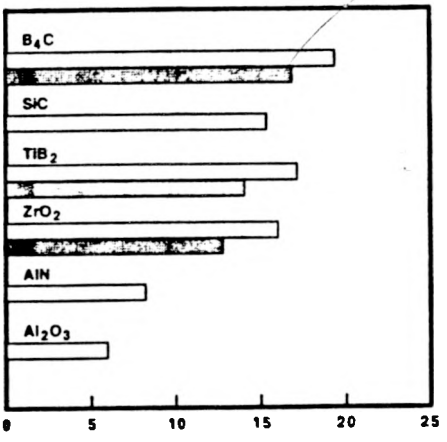


FIGURE 2

Hugoniot elastic limits.

based on an average of two or more experiments. The substantial difference in HEL values for the two boron carbides may reflect the substantially different grain sizes, (3 μm for the DOW material versus 10 μm for the Eagle Picher material). High impurity content in the Eagle Picher material may also play a role. The HEL for silicon carbide is approximately twice the 8 GPa value reported by Gust et al[4]. It is speculated that this is due to the substantially lower silica content of modern silicon carbides.

The HEL values for titanium diboride reported in Figure 2 are tentative. A minor material relaxation observed in the wave profile data at about 6 to 7 GPa is not consistent with onset of pervasive yielding. The data, combined with observations in static studies[5] suggest that the lower pressure feature may be a small phase transformation, while the higher pressure value corresponds to the usual concept of a Hugoniot elastic limit. Similar comments can be made for zirconium dioxide. (See the later discussions on phase transformation behavior.)

Density differences and microstructural observation suggest that variations in the tentative HEL values for the two titanium diborides and two zirconium dioxides are due to small differences in porosity. The effect on the HEL values due to small variations in porosity are unexpectedly large.

The HEL of about 8 GPa for aluminum nitride is in good agreement with recent data of Rosenberg et al[6]. The low HEL for alumina reflects the high porosity of the material studied.

3.3 Post-Yield Strength

Although the Hugoniot elastic limit identifies initial yield in the ceramic and provides an approximate estimate of the initial material strength, assuming that it accurately characterized the subsequent or post-yield strength can be seriously in error. For example silicon carbide and boron carbide have similar HEL's. Subsequent deformations, however, differ markedly. Strength in silicon carbide increases with further deformation, while strength in the boron carbide relaxes dramatically.

Strength at the Hugoniot or peak stress state can be determined by comparing the axial stress and mean stress. We are currently estimating the mean stress behavior by extrapolation of ultrasonic moduli and approximate nonlinear expressions. The difference between the axial and the mean stress state determines the shear strength. Increasing the amplitude of the Hugoniot stress increases the deformation shear strain.

Shear strength versus shear strain data for four of the ceramics studied are shown in Figure 3. Most of the materials indicate neutral or increasing strength with shear deformation. Boron carbide is unique in showing a dramatic loss of strength in post-yield flow. The reasons for the unusual behavior of boron carbide are not known. It may be related to the unusual boron crystal structure and three-body covalent bonding in this material. These are known to produce unusual behavior in other material properties of this ceramic[7].

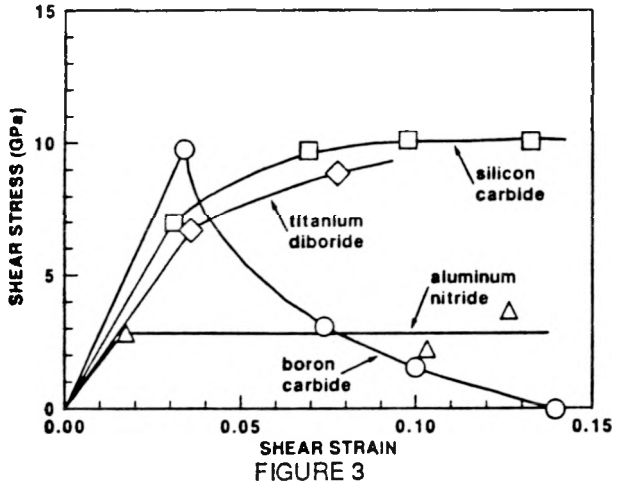

FIGURE 3

Post-yield strength.

3.4 Phase Transformation

Possible phase transformations have been identified in three of the six ceramics tested. These are aluminum nitride, titanium diboride and zirconium dioxide. Interferometer wave profile data for these three ceramics all show a compressive three-wave structure. Aluminum nitride shows a first wave amplitude (Hugoniot elastic limit) at about 8 GPa and a second wave amplitude of approximately 20 GPa. The slow shock velocity of this third wave suggests a large volume change transformation. A possible transition at this Hugoniot pressure has been reported by Kondo et al[8].

First and second wave amplitudes in titanium diboride of approximately 7 GPa and 16 GPa are observed. Shock velocity following the 16 GPa amplitude is more consistent with pervasive plastic flow. Static studies on titanium diboride by Mazurenko et al.[5] suggest that the 7 GPa relaxation may be a small volume change phase transformation although this observation needs to be verified. A complex two-mechanism yield process cannot be ruled out.

In zirconium dioxide first and second wave amplitudes of about 15 GPa and 30 GPa are seen in the compressive wave profile[9]. Again, the second wave velocity is not consistent with full plastic behavior and it is difficult to determine with confidence whether yield precedes phase transformation or the converse.

3.5 Spall Properties

An investigation of the spall properties of high-strength ceramics has been initiated and a revealing base of material property data is emerging. Tensile spall is caused in a planar impact experiment by first precompressing the ceramic sample upon impact. Release waves originating at interfaces between impact ceramic and foam, and between target ceramic and laser window, converge within the target ceramic causing

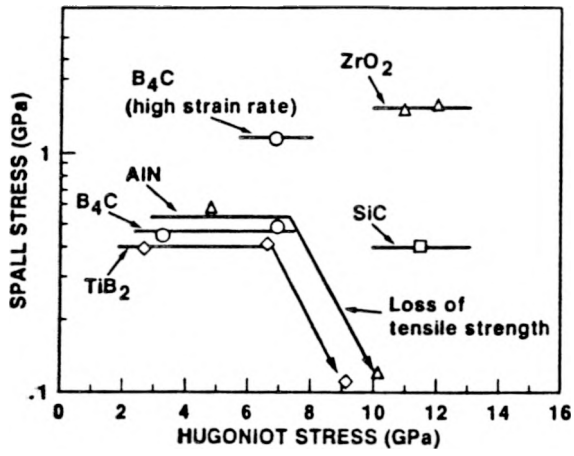


FIGURE 4

Tensile spall properties.

rapid transient tension. If the dynamic tensile strength of the ceramic is exceeded, failure occurs. The signature of the precompression, tension and spall process is transmitted to the ceramic-window interface and recorded in the release portion of the measured wave profile. The strain rate associated with the spall process is determined from the slope of the decompression curve. Kinetics of the spall process are reflected in the shape of the spall pullback signal.

The spall data acquired are summarized in Figure 4. The plot correlates measured spall strength and the precompression stress corresponding to the same data point. Spall strengths under comparable experimental conditions for titanium diboride, boron carbide, silicon carbide and aluminum nitride are similar, ranging from about 0.4 to 0.6 GPa. The high spall strength of zirconium dioxide is presumably due to the transformation toughening mechanism in this material. Precompression of aluminum nitride above 8 GPa Hugoniot elastic limit results in a negligible spall strength measurement. Similarly, precompression of titanium diboride above the suggested 6 to 7 GPa displacive phase change results in a significantly reduced spall strength. Apparently both mechanisms (yielding and phase transformation) result in a degree of compressive fracture which degrades the material tensile strength.

Experiments were designed such that spall occurred at a strain rate of approximately $10^5$/s. One experiment on boron carbide, because of different design and the nondispersive elastic nature of this ceramic, led to spall at a strain rate about an order of magnitude higher. The spall strength was about a factor of two higher (see Figure 6). This datum argues for rate dependence of the tensile spall strength in ceramics which has been noted in previous studies in other brittle materials[10].

## REFERENCES


1. J. J. Gilman, J. Appl. Phys. 41 (1970) 1664.
2. F. L. Addessio and J. N. Johnson, J. Appl. Phys. 67 (1990) 3275.
3. L. M. Barker and R. E. Hollenbach, J. Appl. Phys. 43 (1972) 4669.
4. W. H. Gust, A. C. Holt and E. B. Royce, J. Appl. Phys. (1973) 550.
5. A. M. Mazurenko, V. S. Urbanovich and V. D. Ianovich, Fiz.Tekh. Vys. Davlenii (in Rusian) 21 (1986) 3.
6. Z. Rosenberg, N. S. Brar and S.J. Bless, Univ. Dayton Tech. Rept. UDR-TR-89-74, (1990).
7. D. Emin, Phys. Today 1 (1987) 1.
8. K. Kondo, A. Sawaoka, K. Sato and M. Ando, Shock compression and phase transformation of AlN and BP, In: Shock Waves In Condensed Matter - 1981, eds. W. Nellis et al. (Amer. Inst. Phys., 1982) pp. 325-329.
9. D. Grady and T. Mashimo (in preparation).
10. D. Grady and J. Lipkin, Geophys. Res. Lett., 7 (1980) 255.